Since January 2020 Elsevier has created a COVID-19 resource centre with free information in English and Mandarin on the novel coronavirus COVID-19. The COVID-19 resource centre is hosted on Elsevier Connect, the company's public news and information website.

Elsevier hereby grants permission to make all its COVID-19-related research that is available on the COVID-19 resource centre - including this research content - immediately available in PubMed Central and other publicly funded repositories, such as the WHO COVID database with rights for unrestricted research re-use and analyses in any form or by any means with acknowledgement of the original source. These permissions are granted for free by Elsevier for as long as the COVID-19 resource centre remains active.

Chemical Engineering Journal 405 (2021) 126658

Contents lists available at ScienceDirect

Chemical Engineering Journal

journal homepage: www.elsevier.com/locate/cej

Valorization of disposable COVID-19 mask through the thermo-chemical process

Sungyup Jung[a], Sangyoon Lee[a], Xiaomin Dou[b], Eilhann E. Kwon[a,*]

[a] Department of Environment and Energy, Sejong University, Seoul 05006, Republic of Korea
[b] College of Environmental Science and Engineering, Beijing Forestry University, Beijing 100083, China

HIGHLIGHTS

- A sustainable platform for COVID-19 PPE and CO_2 to syngas was studied.
- Chemical composition and thermal stability of face mask waste were identified.
- Ni catalyst promoted syngas production from pyrolysis of disposable face mask.

GRAPHICAL ABSTRACT

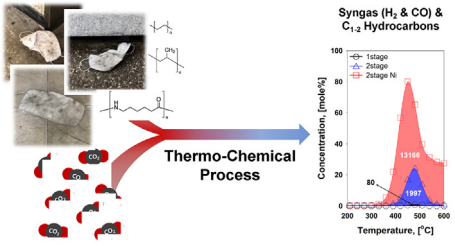

ARTICLE INFO

Keywords:
COVID-19
Face mask
Disposable plastic waste
Hydrogen
Carbon dioxide
Pyrolysis

ABSTRACT

It becomes common to wear a disposable face mask to protect from coronavirus disease 19 (COVID-19) amid this pandemic. However, massive generations of contaminated face mask cause environmental concerns because current disposal processes (*i.e.,* incineration and reclamation) for them release toxic chemicals. The disposable mask is made of different compounds, making it hard to be recycled. In this regard, this work suggests an environmentally benign disposal process, simultaneously achieving the production of valuable fuels from the face mask. To this end, CO_2-assisted thermo-chemical process was conducted. The first part of this work determined the major chemical constituents of a disposable mask: polypropylene, polyethylene, nylon, and Fe. In the second part, pyrolysis study was employed to produce syngas and C_{1-2} hydrocarbons (HCs) from the disposable mask. To enhance syngas and C_{1-2} HCs formations, multi-stage pyrolysis was used for more C–C and C–H bonds scissions of the disposable mask. Catalytic pyrolysis over Ni/SiO_2 further expedited H_2 and CH_4 formations due to its capability for dehydrogenation. In the presence of CO_2, catalytic pyrolysis additionally produced CO, while pyrolysis in N_2 did not produce it. Therefore, the thermo-chemical conversion of disposable face mask and CO_2 could be an environmentally benign way to remove COVID-19 plastic waste, generating value-added products.

1. Introduction

Highly contagious coronavirus disease 19 (COVID-19) was identified/characterized in 2019 [1]. World health organization (WHO) manifested COVID-19 outbreak as pandemic on March 2020 [2] because COVID-19 infects over millions of people in all continents [3]. Under these circumstances, non-pharmaceutical intervention to physically cut off COVID-19 contagion by gearing up a personal protective equipment (PPE) (*e.g.,* mask, glove, protective gown, *etc.*) is mandated in most countries [4–7]. Accordingly, the demands for PPE have been increased [8], which has led to the subsequent generation of plastic wastes [9–11]. Unfortunately, a reliable disposal platform for PPE has

* Corresponding author.
E-mail address: ekwon74@sejong.ac.kr (E.E. Kwon).

https://doi.org/10.1016/j.cej.2020.126658
Received 9 July 2020; Received in revised form 9 August 2020; Accepted 11 August 2020
Available online 14 August 2020
1385-8947/ © 2020 Elsevier B.V. All rights reserved.

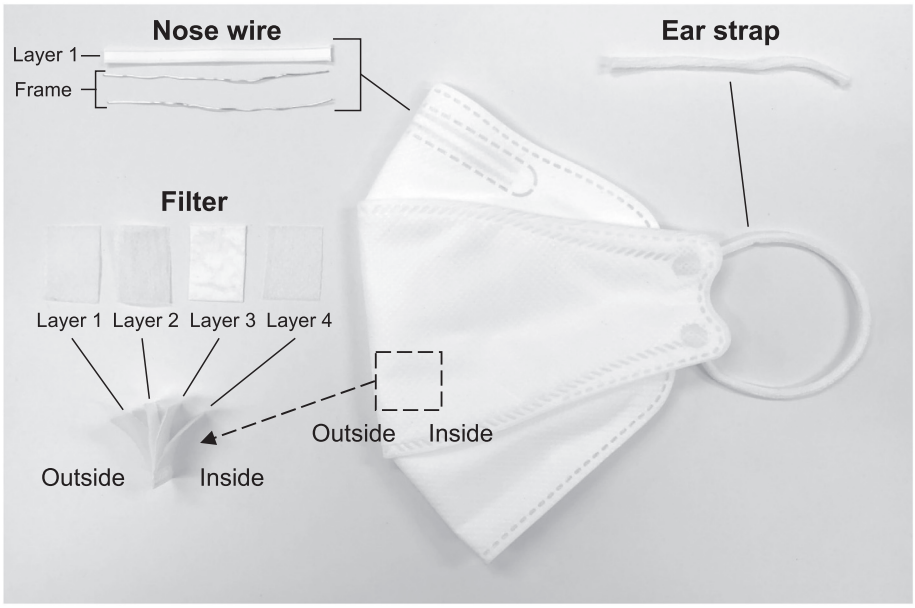

Fig. 1. A photograph of disposal face mask disassembled into different parts.

not been achieved due to several reasons [12]. First of all, most of the disposable face masks used in highly contaminated areas such as medical centers, public transportations, and public places could have high risks of contaminations with coronavirus. In addition, the heterogeneous nature of PPE makes it difficult to establish a reliable recycle platform [13]. Indeed, PPE is manufactured from various polymers (polystyrene, polypropylene, polyethylene, polyvinyl chloride, polyethylene terephthalate, *etc*.) and metallic compounds [9–11]. Despite that recycling is the best disposal option for PPE, such practice is not easily realized due to difficulty in proper separation [14]. Also, upcycling of PPE cannot be made due to a high bio-hazardous potential [15].

In these contexts, thermal destruction through the thermo-chemical process offers a reliable disposal route for PPE [16,17]. Among the thermo-chemical processes, incinerating PPE is commonly practiced [18], but it suffers from technical incompleteness in terms of air pollution controls (APCs) [19]. At the temperature regimes over the transition state, plastics are melted and volatized [20]. Radical pools created from the thermolysis of polymer, such as polyvinyl chloride (PVC), offer a favorable condition for forming toxic chemicals, such as dioxins [21]. Under these conditions, controlling the stoichiometric ratio of fuel to oxygen is challenging, which leads to a difficult condition for complete oxidation [22,23]. Given that most air pollutants are combustion byproducts, additional unit operations for APCs are required to meet the stringent air quality standard [24,25]. Accordingly, finding a reliable disposal platform for PPE beyond incineration is of great importance [17]. It is desirable to recover energy and valuable chemicals from PPE.

Pyrolysis offers an effective means for recovering energy and chemicals through carbon rearrangement [26]. Specifically, carbonaceous materials made for PPE can turn into different phases of pyrogenic products, including syngas, gaseous/liquid hydrocarbons, and solid residue (char) [27]. Carbon distributions into the three phase pyrolysates are controllable by altering the operational parameters (heating rate, temperature, duration, *etc*.) [28,29] and adopting catalysts during the process [30]. As compared to the case of lignocellulosic biomass, the formation of char from pyrolysis of plastic waste (*e.g.,* PPE) is negligible [31]. Accordingly, carbon distribution of PPE likely designated into gaseous and liquid pyrolysates [32]. It is readily inferred that valorization of PPE through the pyrolysis process is advantageous over that of lignocellulosic biomass in that the more gaseous/liquid pyrolysates can be obtained. To offer more environmentally benign means to valorize PPE, this study particularly choose carbon dioxide (CO_2) as a reaction medium. In short, the mechanistic functionality of CO_2 as soft oxidant was reported in our previous study [33]. Given that CO_2 serves a role to alter the compositional modification of gaseous/liquid pyrolysates [34], this study laid great stress on pyrolysis of PPE. More specifically, pyrolysis of a disposable mask from the CO_2 environment was mainly conducted as a case study. To reinforce the mechanistic functionality of CO_2 during pyrolysis of a disposable mask, earth abundant Ni catalyst was adopted, and all pyrolysates through catalytic pyrolysis were characterized. This catalyst was utilized due to its known catalytic capability for dehydrogenation for H_2 production [35,36]. For fundamental study, the main constituents of a disposable mask were determined through analyses of functional groups, organic/inorganic contents, and thermal stability.

2. Materials and methods

2.1. Chemical reagents

Disposable face masks (KF94 grade: the first-class Korean masks that must meet ≥ 94% filtration efficiency of air pollutants) were purchased from a pharmacy store in Seoul, Korea. Prior to pyrolysis studies, the disposable face mask was cut into small pieces and dried at 100 ℃ overnight to remove moisture. Dichloromethane (> 99.95%), silica support (high purity grade, pore size: 60 Å, particle size: 53–210 μm), low density polyethylene (average MW: 4,000), and isotactic polypropylene (average Mw: 12,000) were obtained from Sigma-Aldrich. Nickel nitrate hexahydrate (> 97.0%) and nitric acid (69.0%) were acquired from Daejung Chemical (Korea). ICP multi-element standard solutions (IV and XVI) were purchased from Merck (Germany). Ultra-high purity (99.999%) N_2 and CO_2 gases, and N_2 balanced H_2 (20 vol% H_2) gas were provided from Rigas (Korea).

2.2. Characterization of disposable face mask

Prior to pyrolysis study of the disposable face mask, its chemical compositions were identified. As shown in Fig. 1, the face mask was disassembled into filter (layers 1 – 4), nose wire (layer 1 cover and metal frame), and ear strap parts. Each plastic part was analyzed with FT-IR spectroscopy (Thermo Scientific Nicolet 380) to identify its

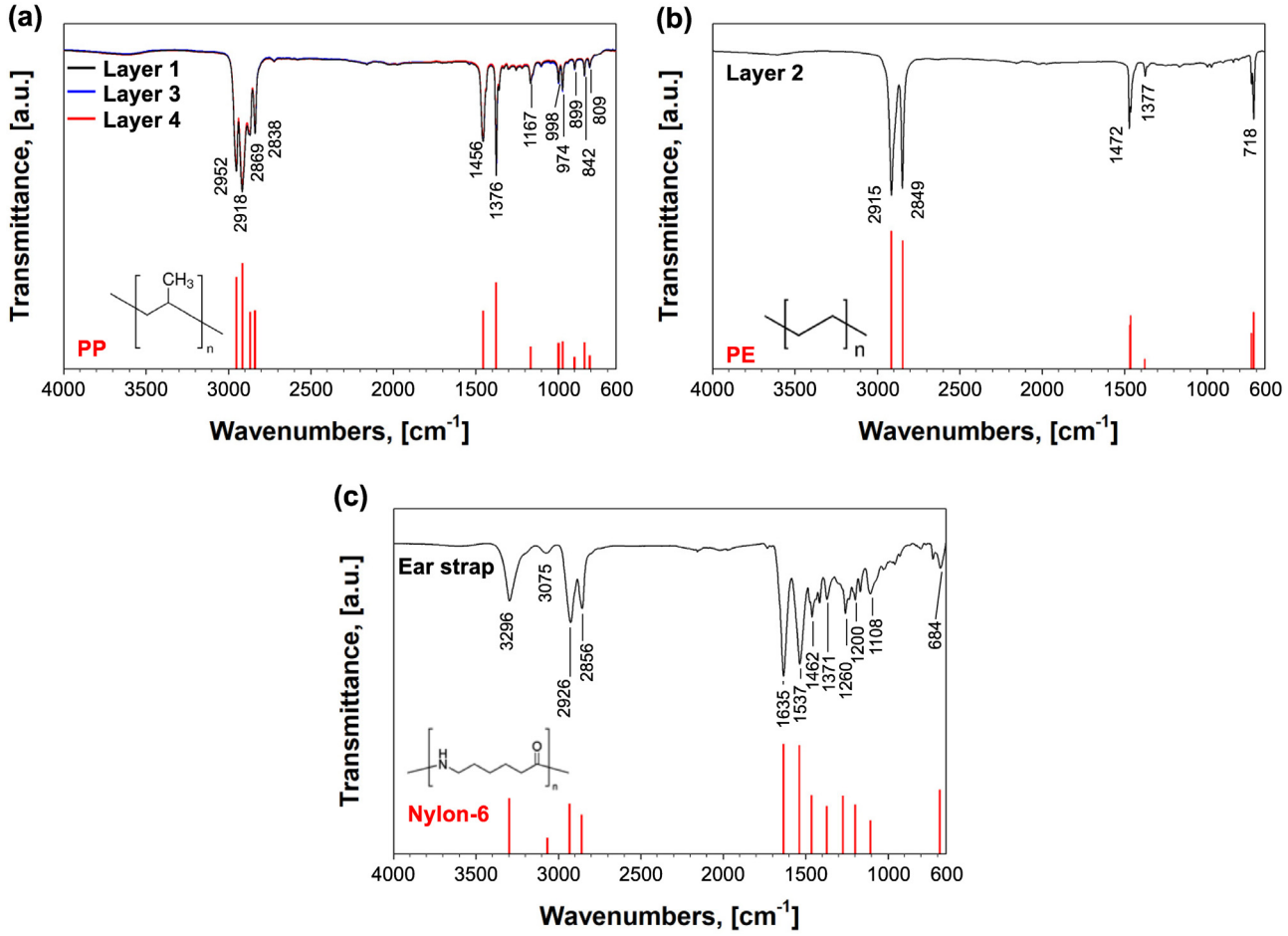

Fig. 2. FT-IR spectra of different plastic parts of a disposable face mask: (a) filter layers 1, 3, and 4, (b) filter layer 2, and (c) ear strap with relevant reference peaks (red bars) of (a) PP [39], (b) PE [40], and (c) nylon-6 [41].

functional groups, while metal frame in the nose wire was quantified with an ICP-OES (Perkin-Elmer Optima 5300 DV). The detailed procedure for ICP-OES is describe elsewhere [37]. To scrutinize the thermolytic profiles of different parts (filter, nose wire, and ear strap) of the disposable face mask, thermo-gravimetric analyses (TGA: Netzsch STA 499) were done under the N_2 and CO_2 environments, varying thermolysis temperature from 35 to 900 ˚C with a constant heating rate (10 ˚C min^{-1}).

2.3. Catalyst preparation and characterizations

Ni/SiO_2 (5 wt% of Ni) was employed as a pyrolysis catalyst in this study. To impregnate Ni metal onto SiO_2 support, wetness incipient impregnation method was adapted. Ni precursor was fully dissolved in deionized water, and the precursor solution was added to the SiO_2 support dropwise. When the impregnation was done, it was placed in a convection oven overnight at 105 ˚C, followed by calcination in the air at 600 ˚C for 5 h. To obtain metal catalyst, the oxidized sample was reduced under 20 vol% of H_2 (N_2 balanced) at 510 ˚C for 4 hr with a heating rate of 2 ˚C min^{-1}. ICP-OES analysis was done to measure the Ni metal loading (4.98 ± 0.02 wt%)

2.4. Experimental setups for disposable face mask pyrolysis

A tubular reactor was assembled with cylindrical furnaces for various pyrolysis experiments (one-stage, two-stage, and catalytic pyrolysis). In the experimental setup for one-stage pyrolysis, 1.00 g (± 0.02) of face mask was inserted into the center of tubular reactor, which operated from 35 to 600 ˚C with a constant heating rate (10 ˚C min^{-1}). In the two-stage pyrolysis, additional furnace (the second heating zone) was placed right next to the first heating zone (furnace operating from 200 to 600 ˚C at 10 ˚C min^{-1}). The second heating zone was operated at a constant temperature (600 ˚C). For catalytic pyrolysis, 5 wt% Ni/SiO_2 (1.00 ± 0.01 g) was added to the second heating zone in the two-stage pyrolysis setup. During pyrolysis in all the experimental setups, either N_2 or CO_2 (100 mL min^{-1}) was flowed through the tubular reactor as a purge gas.

2.5. Product analysis

Gaseous products from face mask pyrolysis were monitored using an on-line micro-GC (3000A, Inficon), directly connected to the tubular reactor. Identification of gaseous products and their quantification were done using a calibration gas mixture (Lot#: 160–401257255-1) made from Inficon. For analysis of condensable hydrocarbons (HCs), a cold solvent trap (-1 ˚C), filled with dichloromethane, was used to condense them. The compositional matrixes of condensed products were analyzed using GC/MS (Agilent 7820A GC and Agilent 5977E MS) and GC/TOF-MS (ALMSCO TOF-MS).

3. Results and discussion

3.1. Identification of the main constituents of face mask

Disposable face masks are manufactured with various plastics (polymers) and inorganic compounds. Given that the disposed face

masks into the environment have no available detailed information on their major constituents, it is required to analyze the types of materials made for them before further treatments. As depicted in the Fig. 1, the disposable face mask was disintegrated into several parts: filter layers 1 – 4, nose wire metal frame, and ear strap. At a glance, it can be realized that filter layers and ear strap are composed of plastics, while nose wire frame is made of metallic compound. Note that plastics are long chain organic carbon-based molecules. Each plastic has their own repeating units, which refer to monomers [38]. To obtain the information on the major repeating units from plastic parts of the face mask, FT-IR was used to characterize functional groups of each part. The resulting FT-IR spectra of plastic parts are shown in the Fig. 2(a) – (c).

The filter layers 1, 3, and 4 showed identical peaks in the two broad ranges from 2838 to 2952 and from 809 to 1456 cm^{-1}, which are characteristic FT-IR peaks of polypropylene (PP) [39]. In contrast, the filter layer 2 had identical peaks at 2915, 2849, 1472, 1377 and 718 with polyethylene (PE) [40]. Ear strap exhibited various peaks with nylon-6 [41]. Nose wire is composed of metal frame and covered by the filter layer 1. The major constituent of the metal frame was Fe (4.58 wt % of total mass of face mask), and the trace amount of other metal species (Zn, Ti, Ca, and Mn) were detected. In Table 1, relative mass portion of plastic and metallic parts of the face mask are summarized with identification of their chemical constituents. The mass portion of different parts of the face mask was measured gravimetrically. In overall, PP (73.33 wt%) and PE (13.77 wt%) are major constituents of the face mask, because they are made for mask filter. Also, nylon (8.27 wt%) and Fe (4.58 wt%) are other main components for ear strap and nose wire frame.

To fundamentally observe the thermolytic profiles of the disposal face mask, TGA test was performed before its pyrolysis study. The TGA measurements were conducted under both the N_2 and CO_2 atmospheres between 35 and 900 °C. Thermolytic profiles of the face mask were plotted as residual mass and differential thermogram (DTG) curves in Fig. 3. Because the negligible thermal degradation (mass change) was shown below 200 °C and above 600 °C, the mass loss and DTG curves were selectively described from 200 to 600 °C. Thermolytic patterns of the face mask were compared with those of two major constituents (*i.e.,* PP and PE) of the face mask (Fig. 3(a)). Major thermal degradation of the face mask initiated around 330 °C and ended up at 495 °C. These start and end temperatures were positioned between those of PP and PE. This is plausible because the major constituents of the face mask are PP and PE as defined in the Fig. 1 and Table 1. The residual mass of 5.28 wt% at 600 °C in the N_2 condition indicates the existence of inorganic compounds, which are of Fe primarily, and small amounts of Zn, Ti, Ca, and Mn.

The TGA results of the face mask under the CO_2 atmosphere was also compared in reference to N_2 environment to determine the impact of CO_2 on face mask pyrolysis (Fig. 3(b)). TGA results under the both conditions showed the identical thermolytic patterns, confirming that no additional heterogeneous reactions between CO_2 and the solid face mask were occurred. Note that the Boudouard reaction (BR) is a thermodynamically preferred heterogeneous reaction between gas phase CO_2 and solid carbon at ≥ 710 °C [42]. Since there was negligible amount of solid carbon left at ≥ 500 °C, the BR could not occur according to the TGA study.

It should be noted that any gas phase reactions from face mask pyrolysis could not be elucidated due to instrumental limitations of TGA unit. Also, gaseous products evolved from face mask pyrolysis were not able to be clarified with the TGA unit, because TGA study only offers a mass change at the given thermolysis temperature ranges. Thus, further studies to reveal the gaseous and liquid products should be performed to understand the thermolysis mechanism of the face mask and the resulting products from it.

Table 1
Chemical compositions of disposable face mask identified by FT-IR and ICP-OES.

Parts	Chemical compositions	Weight percentage (wt.%)
Filter layers 1, 3, 4	PP	73.33
Filter layer 2	PE	13.77
Ear strap	Nylon	8.27
Nose frame	Metals	4.63 (Fe: 4.58, Zn: 0.02, Ti: 0.01, Ca: 0.01, and Mn: 0.01)

3.2. Non-catalytic pyrolysis of disposable face mask

To identify the gaseous effluents from the mask pyrolysis, experimental setup for a single stage (one-stage) pyrolysis was established. The disposable face mask (1 g) was loaded into the tubular reactor within the temperature-programmed tubular furnace (35 to 600 °C at 10 °C min^{-1}) under both the N_2 and CO_2 environments. This temperature program was chosen to match with that of TGA study to identify the thermolysis mechanism of the face mask. The resulting gaseous effluents (H_2, CH_4, C_2H_6, and C_2H_4) are displayed as a function of pyrolysis temperature in the Fig. 4.

From mask pyrolysis, small quantities (< 0.6 mol%) of H_2 and C_{1-2} hydrocarbons (HCs) were detected between 390 and 600 °C under both the N_2 and CO_2 conditions. Also, there was no notable difference shown between them. These results were contrast to the TGA result (Fig. 3), which indicated the substantial thermal degradation of the face mask between 320 and 490 °C. The mass loss of the face mask at this temperature range from the TGA study indicates the evolution of gaseous effluents. In fact, the production of H_2 and C_{1-2} HCs from face mask pyrolysis was up to two orders of magnitude lower than that of other lignocellulosic biomass [43–45]. From the FT-IR analyses, it was confirmed that the main constituents of the face mask are PP, PE, and nylon. The repeating units of PP, PE, and nylon are propylene, ethylene, and long-chain amides, respectively. Therefore, it is estimated that volatile fraction of these plastics is indeed higher than that of lignocellulosic biomass [46,47] because the plastics did not produce a char at 600 °C as demonstrated in the TGA study (Fig. 3). However, the concentration of gaseous effluents from mask pyrolysis was lower. Thus, it can be inferred that the formation of long-chain HCs was occurred after face mask pyrolysis using this single-stage setup.

To confirm the presence of the long-chain HCs from one-stage pyrolysis, condensable HCs evolved from mask pyrolysis were collected through a cold solvent trap, filled with a dichloromethane at low temperature (– 1 °C). The chemical compositions of the condensed gaseous products from one-stage pyrolysis were analyzed using GC-TOF/MS. Fig. 5 and Table 2 represent the compositional matrixes of condensable pyrolysates. Major chemical constituents obtained from face mask pyrolysis were C_{9-46} HCs. Both the N_2 and CO_2 conditions showed similar chromatogram patterns. This confirmed that face mask pyrolysis led to thermal degradation of plastics into long-chain condensable HCs, but it did not fully convert long-chain HCs into H_2 and C_{1-2} HCs. In addition, the effectiveness of CO_2 was not observed under the one-stage pyrolysis.

To enhance the conversion of condensable HCs into more value-added gaseous products (H_2 and C_{1-2} HCs), pyrolysis setup was modified. For more thermal cracking, additional furnace was installed right next to the one-stage pyrolysis setup. The second furnace (second heating zone) operated at 600 °C isothermally, while the first heating zone operated from 35 to 600 °C with a heating rate of 10 °C min^{-1}. The gaseous pyrolysates produced from two-stage pyrolysis are shown in the Fig. 6. From the two-stage pyrolysis the formations of H_2 (3.5 mol %), CH_4 (12.0 mol%), C_2H_6 (4.8 mol%), and C_2H_4 (9.5 mol%) were substantially enhanced from results of one-stage pyrolysis (< 0.6 mol% of H_2 and C_{1-2} HCs) under the N_2 condition. This result well agreed with the hypothesis that condensable HCs can be converted into gaseous HCs with additional thermal energy. Considering that chemical structures of

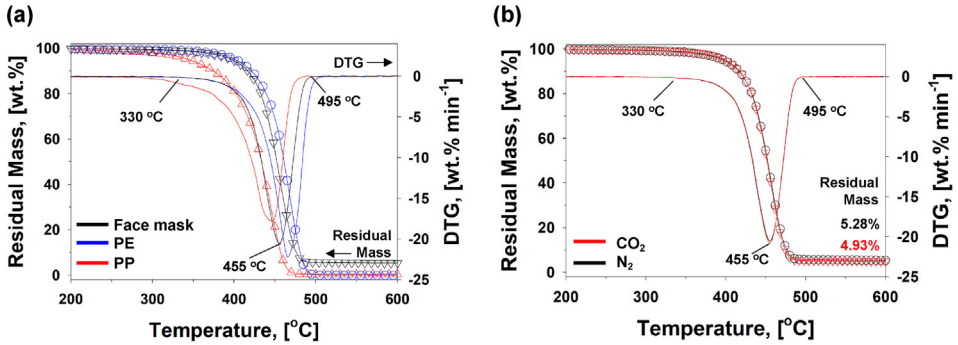

Fig. 3. (a) Mass loss and DTG curves of face mask, PP, and, low density PE between 200 and 600 ℃ under the N_2 environment, and (b) mass loss and DTG curves of face mask under the N_2 and CO_2 environments.

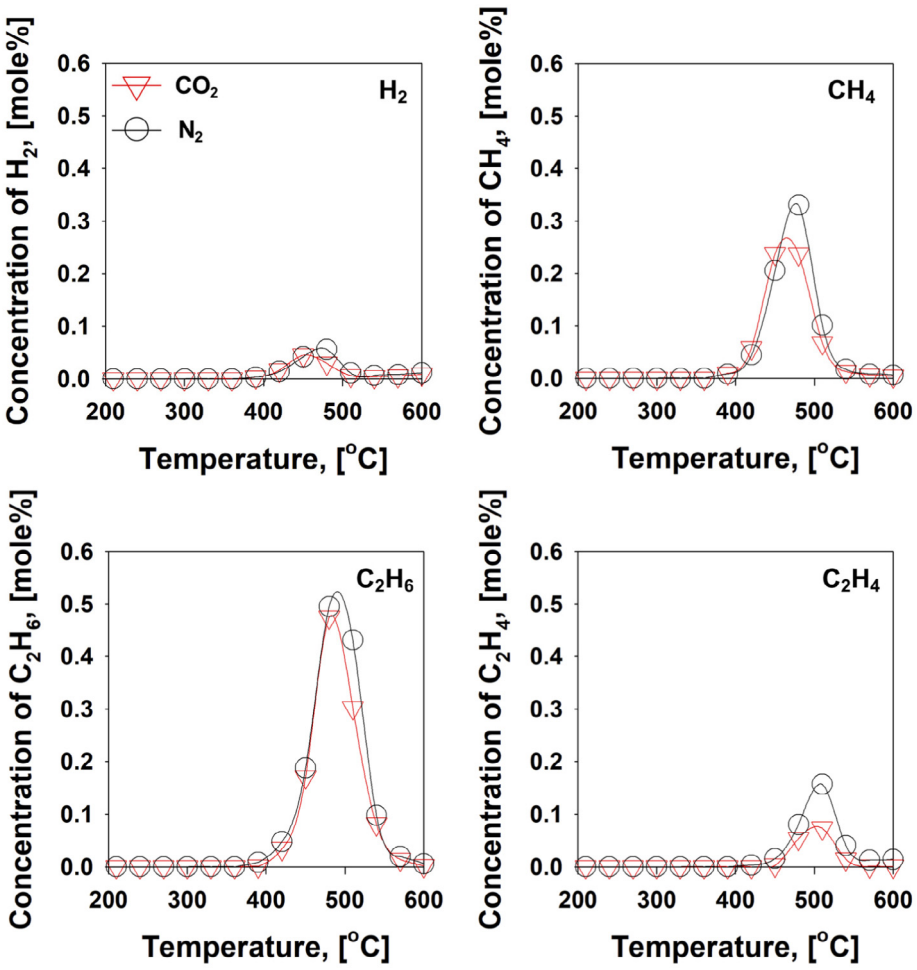

Fig. 4. Gas evolution profiles from mask pyrolysis with one-stage setup under the N_2/CO_2 atmospheres.

PP, PE, and nylon are mostly composed of C–C and C–H bonds [48], the thermal energy through the second heating zone significantly contributed to the improvement of reaction kinetics for C–C and C–H bonds scissions for the production of gaseous effluents (H_2 and $C_{1\text{-}2}$ HCs). The production of $C_{1\text{-}2}$ HCs was likely due to the C–C bond scissions [48], while the production of H_2 was attributed to C–H bond scissions [49]. The results of pyrolysis studies of the disposable face mask were identical in both the N_2 and CO_2 environments. This offers that CO_2 can be a viable purge gas for pyrolysis of the plastic waste in the replacement of the conventional purge gas, N_2.

3.3. Catalytic pyrolysis of disposable face mask

As discussed in the TGA experiments (Fig. 2 and Table 1), the disposable face mask contained higher than 95 wt% of volatile compounds (PP, PE, and nylon), which are mostly composed of C–C and C–H bonds. As a means to enhance the reaction kinetics for C–C and C–H bonds scissions, additional heating zone was introduced in the two-stage pyrolysis. Although the two-stage pyrolysis substantially improved the C–C and C–H bonds scissions with the formations H_2 and $C_{1\text{-}2}$ HCs, there was still remained long-chain HCs. Also, much higher concentrations of $C_{1\text{-}2}$ HCs than the H_2 were shown. These indicate that the further C–C and C–H bonds scissions of various HCs can facilitate H_2 formations. For this reason, Ni-based catalyst (Ni/SiO_2) was employed to conduct

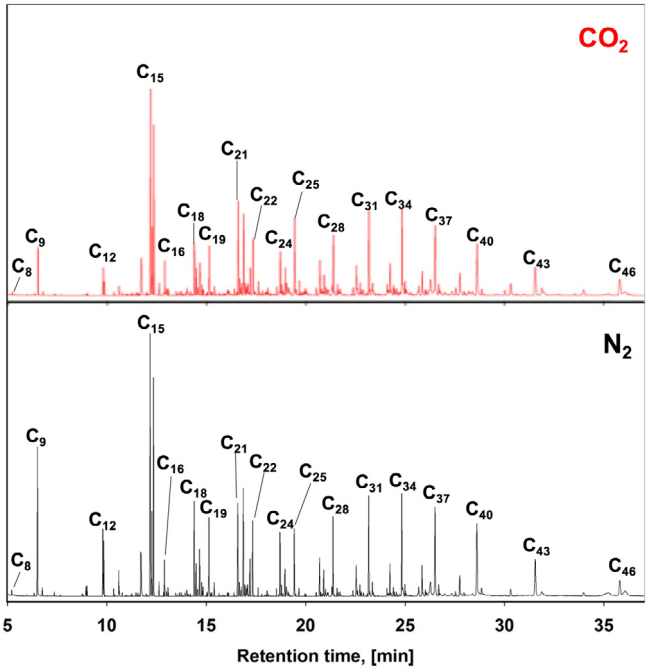

Fig. 5. GC-TOF/MS results of condensable HCs obtained from mask pyrolysis under the N_2/CO_2 atmospheres.

catalytic pyrolysis of the face mask in the two-stage setup. Ni catalyst was selected because of its known catalytic performance for C–H bond scissions (dehydrogenation for H_2 production) [36,50,51]. The evolution profiles of gaseous pyrolysates (H_2, CH_4, CO, C_2H_6, and C_2H_4) from catalytic pyrolysis against first heating zone temperature are plotted in Fig. 7.

Under the N_2 environment, the performance of catalytic pyrolysis over Ni/SiO_2 was much greater than non-catalytic pyrolysis. In detail, the maximum concentration of H_2 increased from 3.5 to 55.1 mol%, and that of CH_4 increased from 12.0 to 18.2 mol%. In contrast, the concentrations of C_2 HCs were reduced. Thus, it is inferred that C–H and C–C bond scissions of C_2 and longer chain HCs over Ni/SiO_2 catalyst contributed to H_2 and CH_4 formations. The dominant production of H_2 over other HCs indicates that Ni catalyst selectively contributed to C–H bond scissions over C–C bond scissions.

In the CO_2 environment, the similar evolution trends were shown, which are dominant production of H_2 and CH_4 with the reduction of C_2H_6 and C_2H_4 formations (Fig. 7). Nonetheless, concentrations of H_2 and $C_{1\text{-}2}$ HCs were relatively lower, comparing to the results in the N_2 condition. The most noticeable difference of catalytic pyrolysis under the CO_2 with other pyrolysis setups was CO formation as a major gaseous product. Because of the major constituents of the face mask (*i.e.*, PP, PE, and nylon) have limited quantity of oxygen, the high quantity of CO cannot be expected without the presence of CO_2 as an oxygen source. As discussed in the TGA result, the heterogeneous reaction (*i.e.*, BR) between gaseous CO_2 and solid carbon could not occur at this temperature region. Therefore, there are three possibilities to produce CO in the presence of CO_2 over Ni/SiO_2 catalyst: (1) reverse water–gas-shift (RWGS) reaction ($H_2 + CO_2 \rightleftharpoons CO + H_2O$), (2) CO_2 dry reforming (*e.g.*, $CH_4 + CO_2 \rightleftharpoons 2H_2 + 2CO$), and (3) gas phase homogeneous reactions (GPRs) between CO_2 and gaseous HCs evolved from the face mask pyrolysis through the second heating zone at 600 ℃. The first suggestion is closely related to the presence of both H_2 and CO_2. Indeed, the concentration of H_2 was reduced at ≥ 330 ℃ in the presence of CO_2, comparing to N_2 condition. This temperature range was overlapped with the temperature window for CO production. In addition, CO_2 dry reforming also could be plausible due to the reduction of CH_4 concentration in the presence of CO_2, comparing to the pyrolysis result in the N_2 condition. Since both the RWGS and CO_2 dry reforming reactions produce CO, consuming H_2 and CH_4, the total molar concentrations of H_2, CO, and CH_4 should be matched when only these two reactions were occurred for CO formation (Fig. 7). However, higher concentrations of gaseous effluents were observed in the CO_2 condition than the N_2 condition (Fig. 7). Thus, it can be inferred that CO formation was not entirely ascribed to the RWGS and CO_2 dry reforming, thereby suggesting additional GPRs between CO_2 and gaseous HCs evolved from face mask pyrolysis. In other words, CO_2 acted as a soft oxidant for catalytic pyrolysis of the face mask over Ni/SiO_2. Therefore, the second highest peak of CO shown at 480 ℃ was likely ascribed to the GPRs (Fig. 7). Through the catalytic pyrolysis, the cumulative production of gaseous effluents increased 25 times and 165 times higher than two-stage pyrolysis and one-stage pyrolysis, respectively, under the CO_2

Table 2
Peaks areas of chemical constituents obtained from condensable HCs under N_2 and CO_2 atmospheres.

Peak Notation	Component	Retention Time	Molecular Weight	Area (CO_2) × 10^{-6}	Area (N_2) × 10^{-6}
C_8	4-methylheptane	5.222	114	1.09	1.45
C_9	2,4-Dimethyl-1-heptene	6.517	126	18.54	38.19
C_{12}	2,4,6-trimethyl-1-nonene (meso form)	9.804	168	7.29	15.04
	2,4,6-trimethyl-1-nonene (racemic form)	9.853	168	5.38	11.50
C_{15}	2,4,6,8-tetramethyl-1-undecene (isotactic)	12.180	210	47.54	58.80
	2,4,6,8-tetramethyl-1-undecene (heterotactic)	12.266	210	17.81	21.28
	2,4,6,8-tetramethyl-1-undecene (syndiotactic)	12.353	210	39.56	49.43
C_{16}	2,4,6,8,10-pentamethyl-1,10-undecadiene (isotactic)	12.909	222	8.66	84.17
C_{18}	2,4,6,8,10-pentamethyl-1-tridecene (isotactic)	14.391	252	18.19	22.73
C_{19}	2,4,6,8,10,12-hexamethyl-1,12-tridecadiene (isotactic)	15.139	264	14.44	20.57
C_{21}	2,4,6,8,10,12-hexamethyl-1-pentadecene (isotactic)	16.588	294	26.38	24.75
C_{22}	2,4,6,8,10,12,14-heptamethyl-1,14-pentadecadiene (isotactic)	17.335	306	22.86	19.36
C_{24}	2,4,6,8,10,12,14-heptamethyl-1-heptadecene (isotactic)	18.713	336	15.71	17.52
C_{25}	2,4,6,8,10,12,14,16-octamethyl-1,16-heptadecadiene (isotactic)	19.429	348	26.93	19.38
C_{28}	2,4,6,8,10,12,14,16,18-nonamethyl-1,18-nonadecadiene (isotactic)	21.378	390	22.35	21.34
C_{31}	2,4,6,8,10,12,14,16,18,20-decamethyl-1,20-henicosadiene (isotactic)	23.174	432	24.45	27.49
C_{34}	2,4,6,8,10,12,14,16,18,20,22-undecamethyl-1,22-tricosadiene(isotactic)	24.831	474	33.27	30.14
C_{37}	2,4,6,8,10,12,14,16,18,20,22,24-dodecamethyl-1,24-pentacosadiene (isotactic)	26.504	516	32.95	34.64
C_{40}	2,4,6,8,10,12,14,16,18,20,22,24,26-tridecamethyl-1,26-heptacosadiene (isotactic)	28.608	558	26.77	33.42
C_{43}	2,4,6,8,10,12,14,16,18,20,22,24,26,28-tetradecamethyl-1,28-nonacosadiene (isotactic)	31.884	600	21.23	25.84
C_{46}	2,4,6,8,10,12,14,16,18,20,22,24,26,28,30-pentadecamethyl-1,30-untriacontadiene (isotactic)	35.802	642	15.95	22.12

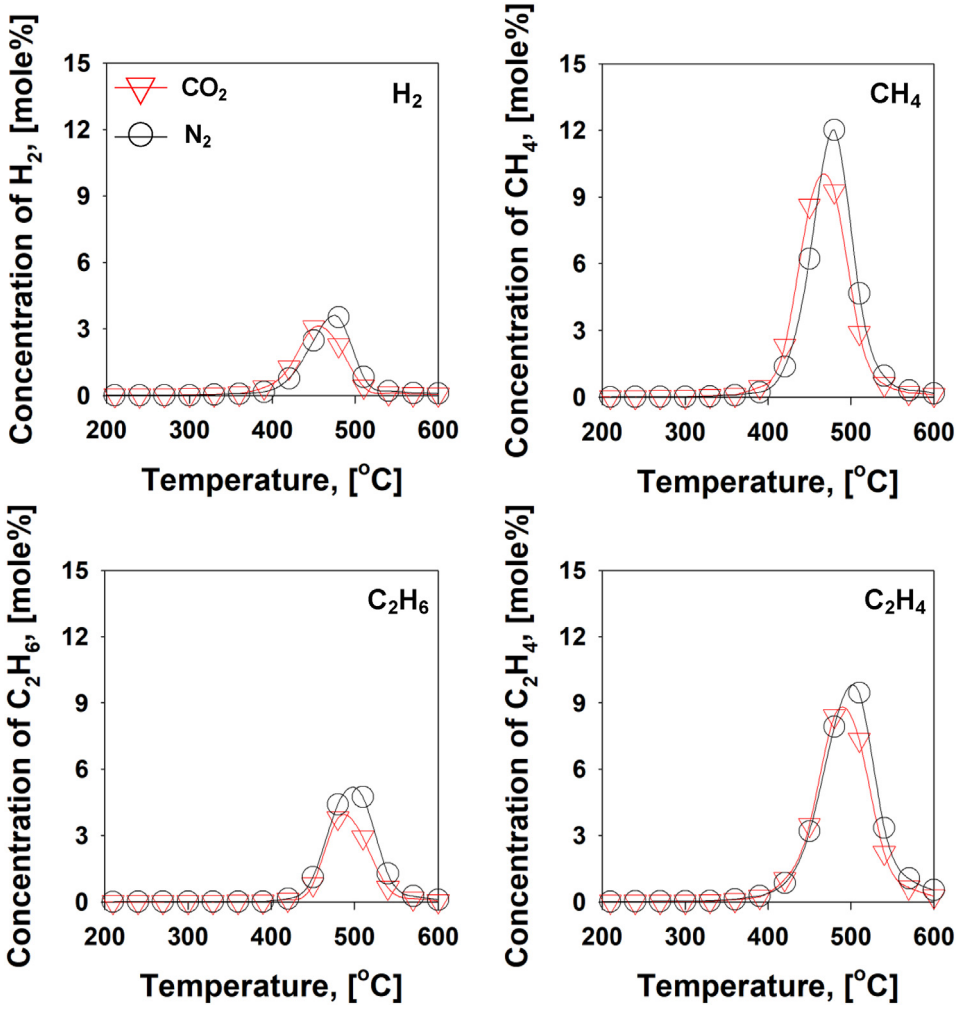

Fig. 6. Gas evolution profiles from mask pyrolysis with two-stage setup under the N_2/CO_2 atmospheres.

condition (Fig. 8).

By switching purge gases of the face mask catalytic pyrolysis between N_2 and CO, different H_2/CO ratio was achieved from the face mask catalytic pyrolysis (Fig. 7). This immediate control of H_2/CO ratios can be technically and industrially beneficial. Both H_2 and CO are useful industrial chemicals and fuels to be used as direct fuels and intermediates for the production of more value-added chemicals through well-defined chemical processes. In the chemical processes, the control of H_2/CO ratios is crucial to selectively produce desired chemicals such as saturated HCs [52], olefins [52], and alcohols [53].

In sum, this work offered a versatile thermo-chemical process to valorize the disposable COVID-19 face mask. To suggest an environmentally benign process, CO_2 was utilized as a reaction medium for pyrolysis of the disposable face mask. Prior to pyrolysis study, chemical constituents of the disposable mask were investigated. Because major compounds of the face mask were plastics (PP, PE, and nylon), its pyrolysis resulted in the production of H_2 and various ranges of HCs. To enhance the generations of value-added H_2 and $C_{1\text{-}2}$ HCs, multi-stage pyrolysis setup was employed for C–C and C–H bonds scissions of long-chain HCs. Further pyrolysis over Ni/SiO_2 catalyst led to substantial conversion of longer chain ($\geq C_2$) HCs into H_2 and CH_4. During catalytic pyrolysis, H_2 production was substantially improved under the N_2 condition, while significant CO formation was shown under the CO_2 environment due to RWGS, CH_4 dry reforming, and gas phase reactions of CO_2. Thus, H_2/CO ratio was controlled in the catalytic pyrolysis when the reaction gas medium was changed. In contrast, CO_2 worked as an inert gas for non-catalytic pyrolysis. These findings offer that CO_2 can be considered a versatile purge gas and soft oxidant in various thermo-chemical processes, controlling exit gaseous effluents. Formations of syngas and $C_{1\text{-}2}$ HCs from plastic waste (disposable face mask) and greenhouse gas (CO_2) can contribute to the reduction of CO_2 emission by counterbalancing fossil fuel production. This also could be an environmentally benign and process-efficient way to dispose of COVID-19 plastic waste, simultaneously generating value-added products.

Declaration of Competing Interest

The authors declare that they have no known competing financial interests or personal relationships that could have appeared to influence the work reported in this paper.

Acknowledgement

This work was also supported by the National Research Foundation of Korea (NRF) grants funded by the Korea government (MSIT) (NRF-2019H1D3A1A01070644 and NRF-2019R1A4A1027795).

Appendix A. Supplementary data

Supplementary data to this article can be found online at https://doi.org/10.1016/j.cej.2020.126658.

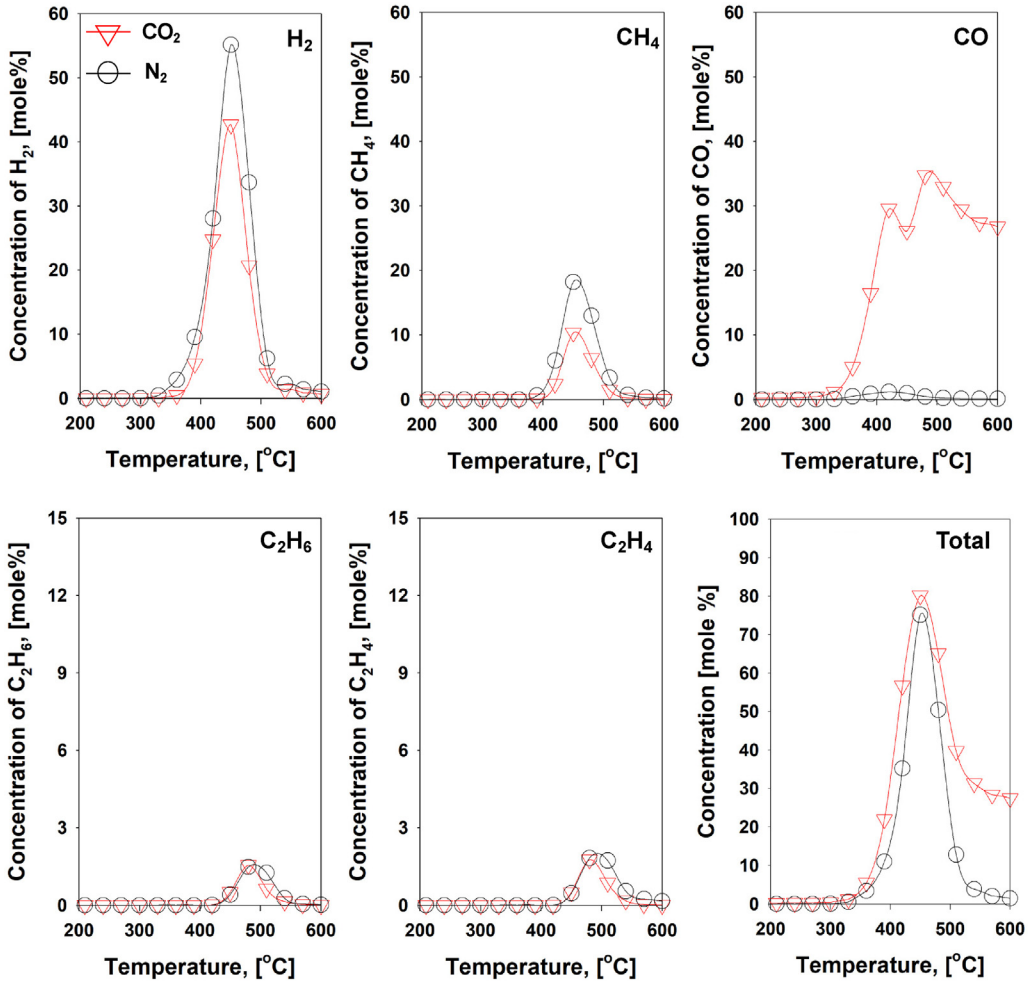

Fig. 7. Gas evolution profiles from mask pyrolysis with 5 wt% Ni/SiO_2 catalyst under the N_2/CO_2 atmospheres.

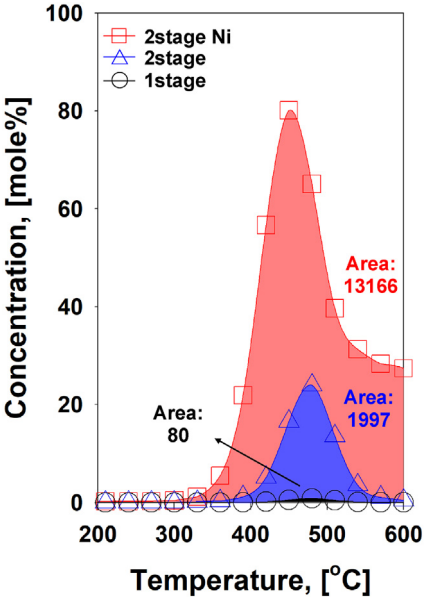

Fig. 8. Comparison of overall gas production from one-stage pyrolysis, two-stage pyrolysis, and catalytic pyrolysis (5 wt% Ni/SiO_2) of the disposal face mask under the CO_2 environment.

References

[1] D.E.L. Promislow, A geroscience perspective on COVID-19 mortality, The journals of gerontology. Series A, Biological sciences and medical sciences (2020).

[2] WHO, WHO Director-General's opening remarks at the media briefing on COVID-19 - 11 March 2020, 2020.

[3] WHO, Coronavirus disease (COVID-19). World Health Organization Situation Report – 134, 2020.

[4] CDC, Interim Infection Prevention and Control Recommendations for Patients with Suspected or Confirmed Coronavirus Disease 2019 (COVID-19) in Healthcare Settings (Centers for Disease Control and Prevention: CDC), 2020.

[5] PHAC, Coronavirus disease (COVID-19): For health professionals (Public Health Agency of Canada: PHAC), 2020.

[6] WHO, Rational use of personal protective equipment for coronavirus disease 2019 (COVID-19) - World Health Organization (WHO), 2020.

[7] ECDC, Guidance for wearing and removing personal protective equipment in healthcare settings for the care of patients with suspected or confirmed COVID-19 (European Center for Disease Prevention and Control: ECDC), 2020.

[8] J.J. Klemeš, Y.V. Fan, R.R. Tan, P. Jiang, Minimising the present and future plastic waste, energy and environmental footprints related to COVID-19, Renew. Sustain. Energy Rev. 127 (2020) 109883.

[9] K. Aalto-Korte, L. Ackermann, M.L. Henriks-Eckerman, J. Välimaa, H. Reinikka-Railo, E. Leppänen, R. Jolanki, 1,2-Benzisothiazolin-3-one in disposable polyvinyl chloride gloves for medical use, Contact Dermatitis 57 (2007) 365–370.

[10] S. Lee, A.R. Cho, D. Park, J.K. Kim, K.S. Han, I.J. Yoon, M.H. Lee, J. Nah, Reusable Polybenzimidazole Nanofiber Membrane Filter for Highly Breathable PM 2.5 Dust Proof Mask, ACS Appl. Mater. Interfaces 11 (2019) 2750–2757.

[11] S. Aslan, S. Kaplan, C. Çetin, An investigation about comfort and protection performances of disposable and reusable surgical gowns by objective and subjective measurements, J. Text. Inst. 104 (2013) 870–882.

[12] A. Bdour, B. Altrabsheh, N. Hadadin, M. Al-Shareif, Assessment of medical wastes management practice: A case study of the northern part of Jordan, Waste Manage. 27 (2007) 746–759.

[13] S.-L. Wu, J.-H. Kuo, M.-Y. Wey, Thermal degradation of waste plastics in a two-stage pyrolysis-catalysis reactor over core-shell type catalyst, J. Anal. Appl. Pyrol.

142 (2019) 104641.
[14] S.D. Anuar Sharuddin, F. Abnisa, W.M.A. Wan Daud, M.K. Aroua, A review on pyrolysis of plastic wastes, Energy Convers. Manage. 115 (2016) 308–326.
[15] J. Ma, J. Wang, X. Tian, H. Zhao, In-situ gasification chemical looping combustion of plastic waste in a semi-continuously operated fluidized bed reactor, Proc. Combust. Inst. 37 (2019) 4389–4397.
[16] S.M. Al-Salem, A. Antelava, A. Constantinou, G. Manos, A. Dutta, A review on thermal and catalytic pyrolysis of plastic solid waste (PSW), J. Environ. Manage. 197 (2017) 177–198.
[17] L. Qin, J. Han, B. Zhao, Y. Wang, W. Chen, F. Xing, Thermal degradation of medical plastic waste by in-situ FTIR, TG-MS and TG-GC/MS coupled analyses, J. Anal. Appl. Pyrol. 136 (2018) 132–145.
[18] R. Geyer, J.R. Jambeck, K.L. Law, Production, use, and fate of all plastics ever made, Sci. Adv. 3 (2017).
[19] L. Makarichi, W. Jutidamrongphan, K.-A. Techato, The evolution of waste-to-energy incineration: A review, Renew. Sustain. Energy Rev. 91 (2018) 812–821.
[20] X. Wang, D. Ma, Q. Jin, S. Deng, H. Stančin, H. Tan, H. Mikulčić, Synergistic effects of biomass and polyurethane co-pyrolysis on the yield, reactivity, and heating value of biochar at high temperatures, Fuel Process. Technol. 194 (2019) 106127.
[21] H. Zhao, J. Wang, Chemical-looping combustion of plastic wastes for in situ inhibition of dioxins, Combust. Flame 191 (2018) 9–18.
[22] M.-Y. Wey, L.-J. Yu, S.-I. Jou, The influence of heavy metals on the formation of organics and HCl during incinerating of PVC-containing waste, J. Hazard. Mater. 60 (1998) 259–270.
[23] A. Buekens, K. Cen, Waste incineration, PVC, and dioxins, J. Mater. Cycles Waste Manage. 13 (2011) 190–197.
[24] J.-W. Lu, S. Zhang, J. Hai, M. Lei, Status and perspectives of municipal solid waste incineration in China: A comparison with developed regions, Waste Manage. 69 (2017) 170–186.
[25] M.J. Quina, E. Bontempi, A. Bogush, S. Schlumberger, G. Weibel, R. Braga, V. Funari, J. Hyks, E. Rasmussen, J. Lederer, Technologies for the management of MSW incineration ashes from gas cleaning: New perspectives on recovery of secondary raw materials and circular economy, Sci. Total Environ. 635 (2018) 526–542.
[26] K.G. Burra, A.K. Gupta, Kinetics of synergistic effects in co-pyrolysis of biomass with plastic wastes, Appl. Energy 220 (2018) 408–418.
[27] R. Miandad, M.A. Barakat, A.S. Aburiazaiza, M. Rehan, A.S. Nizami, Catalytic pyrolysis of plastic waste: a review, Process Saf. Environ. Prot. 102 (2016) 822–838.
[28] R.K. Singh, B. Ruj, Time and temperature depended fuel gas generation from pyrolysis of real world municipal plastic waste, Fuel 174 (2016) 164–171.
[29] S. Jung, Y.-K. Park, E.E. Kwon, Strategic use of biochar for CO_2 capture and sequestration, Journal of CO_2 Utilization 32 (2019) 128–139.
[30] D. Yao, C. Wu, H. Yang, Y. Zhang, M.A. Nahil, Y. Chen, P.T. Williams, H. Chen, Co-production of hydrogen and carbon nanotubes from catalytic pyrolysis of waste plastics on Ni-Fe bimetallic catalyst, Energy Convers. Manage. 148 (2017) 692–700.
[31] M.V. Navarro, J.M. López, A. Veses, M.S. Callén, T. García, Kinetic study for the co-pyrolysis of lignocellulosic biomass and plastics using the distributed activation energy model, Energy 165 (2018) 731–742.
[32] S. Kim, C. Park, J. Lee, Reduction of polycyclic compounds and biphenyls generated by pyrolysis of industrial plastic waste by using supported metal catalysts: A case study of polyethylene terephthalate treatment, J. Hazard. Mater. 392 (2020) 122464.
[33] T. Lee, S. Jung, J. Hong, C.H. Wang, D.S. Alessi, S.S. Lee, Y.K. Park, E.E. Kwon, Using CO2 as an Oxidant in the Catalytic Pyrolysis of Peat Moss from the North Polar Region, Environ. Sci. Technol. 54 (2020) 6329–6343.
[34] S.-H. Cho, S.S. Lee, S. Jung, Y.-K. Park, K.-Y.-A. Lin, J. Lee, E.E. Kwon, Carbon dioxide-cofeeding pyrolysis of pine sawdust over nickle-based catalyst for hydrogen production, Energy Convers. Manage. 201 (2019) 112140.
[35] S. Jung, D. Choi, Y.-K. Park, Y. Fai Tsang, N.B. Klinghoffer, K.-H. Kim, E.E. Kwon, Functional use of CO_2 for environmentally benign production of hydrogen through catalytic pyrolysis of polymeric waste, Chem. Eng. J. (2020) 125889.
[36] J. Xu, G.F. Froment, Methane steam reforming, methanation and water-gas shift: I. intrinsic kinetics, AIChE J. 35 (1989) 88–96.
[37] J.-H. Kim, S. Jung, Y.-K. Park, E.E. Kwon, CO_2-cofed catalytic pyrolysis of tea waste over Ni/SiO_2 for the enhanced formation of syngas, J. Hazard. Mater. 396 (2020) 122637.
[38] R. Siddique, J. Khatib, I. Kaur, Use of recycled plastic in concrete: A review, Waste Manage. 28 (2008) 1835–1852.
[39] M.R. Jung, F.D. Horgen, S.V. Orski, V. Rodriguez C, K.L. Beers, G.H. Balazs, T.T. Jones, T.M. Work, K.C. Brignac, S.-J. Royer, K.D. Hyrenbach, B.A. Jensen, J.M. Lynch, Validation of ATR FT-IR to identify polymers of plastic marine debris, including those ingested by marine organisms, Marine Pollution Bulletin 127 (2018) 704-716.
[40] H. Rajandas, S. Parimannan, K. Sathasivam, M. Ravichandran, L. Su Yin, A novel FTIR-ATR spectroscopy based technique for the estimation of low-density polyethylene biodegradation, Polym. Test. 31 (2012) 1094–1099.
[41] K.H. Lee, K.W. Kim, A. Pesapane, H.Y. Kim, J.F. Rabolt, Polarized FT-IR study of macroscopically oriented electrospun nylon-6 nanofibers, Macromolecules 41 (2008) 1494–1498.
[42] E.E. Kwon, E.-C. Jeon, M.J. Castaldi, Y.J. Jeon, Effect of carbon dioxide on the thermal degradation of lignocellulosic biomass, Environ. Sci. Technol. 47 (2013) 10541–10547.
[43] S. Jung, D. Kwon, Y.F. Tsang, Y.-K. Park, E.E. Kwon, CO_2-cofeeding catalytic pyrolysis of macadamia nutshell, Journal of CO_2 Utilization 37 (2020) 97–105.
[44] T. Lee, I.-H. Nam, S. Jung, Y.-K. Park, E.E. Kwon, Synthesis of nickel/biochar composite from pyrolysis of *Microcystis Aeruginosa* and its practical use for syngas production, Bioresour. Technol. 300 (2020) 122712.
[45] E.E. Kwon, T. Lee, Y.S. Ok, D.C.W. Tsang, C. Park, J. Lee, Effects of calcium carbonate on pyrolysis of sewage sludge, Energy 153 (2018) 726–731.
[46] J.H. Park, H.-W. Park, S. Choi, D.-W. Park, Effects of blend ratio between high density polyethylene and biomass on co-gasification behavior in a two-stage gasification system, Int. J. Hydrogen Energy 41 (2016) 16813–16822.
[47] J.-M. Jung, J.-I. Oh, K. Baek, J. Lee, E.E. Kwon, Biodiesel production from waste cooking oil using biochar derived from chicken manure as a porous media and catalyst, Energy Convers. Manage. 165 (2018) 628–633.
[48] X. Liu, X. Li, J. Liu, Z. Wang, B. Kong, X. Gong, X. Yang, W. Lin, L. Guo, Study of high density polyethylene (HDPE) pyrolysis with reactive molecular dynamics, Polym. Degrad. Stab. 104 (2014) 62–70.
[49] Z. Gao, I. Amasaki, T. Kaneko, M. Nakada, Calculation of activation energy from fraction of bonds broken for thermal degradation of polyethylene, Polym. Degrad. Stab. 81 (2003) 125–130.
[50] U. Rodemerck, M. Schneider, D. Linke, Improved stability of Ni/SiO_2 catalysts in CO_2 and steam reforming of methane by preparation via a polymer-assisted route, Catal. Commun. 102 (2017) 98–102.
[51] S. Kim, E.E. Kwon, Y.T. Kim, S. Jung, H.J. Kim, G.W. Huber, J. Lee, Recent advances in hydrodeoxygenation of biomass-derived oxygenates over heterogeneous catalysts, Green Chem. 21 (2019) 3715–3743.
[52] R.A. van Santen, A.J. Markvoort, I.A.W. Filot, M.M. Ghouri, E.J.M. Hensen, Mechanism and microkinetics of the Fischer-Tropsch reaction, PCCP 15 (2013) 17038–17063.
[53] K. Fang, D. Li, M. Lin, M. Xiang, W. Wei, Y. Sun, A short review of heterogeneous catalytic process for mixed alcohols synthesis via syngas, Catal. Today 147 (2009) 133–138.